Modelling navigation in muddy areas

Guillaume Delefortrie, Ghent University, Maritime Technology, Belgium
Marc Vantorre, Ghent University, Maritime Technology, Belgium

Abstract

In navigation areas with bottoms covered by a fluid mud layer, the *nautical bottom* concept is introduced to assess the under keel clearance and the level of dredging. Up till now the nautical bottom has always been defined using the characteristics of the mud layer. However, criteria based on ship behaviour may result in a more efficient definition of the nautical bottom. A mathematical model formulation for ship manoeuvring in muddy areas, based on systematic captive model tests is proposed. Full mission ship manoeuvring simulator runs were carried out to review the nautical bottom concept in the harbour of Zeebrugge, Belgium; a selection of simulation results is presented.

1   Introduction

The last decade the dimensions and capacity of container vessels has increased significantly. In order to maintain their competitive position, it is important for the port authorities to keep their harbour accessible for the largest ships without jeopardising safety of shipping traffic. Especially an increase of draft may cause problems, as a minimal under keel clearance is required, not only to decrease the probability of bottom contact, but also to avoid unacceptable effects on the manoeuvrability of the ship.

The available gross under keel clearance of the ship is known whenever the water depth is. If the bottom of the fairway is covered with a layer of fluid mud, it is more difficult to assess the available under keel clearance, as the physical characteristics of a mud layer – such as density, viscosity, yield stress – vary with the depth. In many areas, the upper part of a mud layer can be considered as a fluid with low density and viscosity; both parameters increase more or less gradually with depth. Often a significant increase of the rheological properties occurs at a certain depth: this is referred to as the *rheological transition*.

It is unlikely that a ship will suffer damage when its keel touches the upper part of the mud layer, as would occur when touching a hard bottom. On the other hand it is likely

that the presence of the mud will modify the manoeuvring behaviour of the ship. In order to define the reference level for maintenance dredging works and for estimating the available under keel clearance in muddy areas, the *nautical bottom* is defined as *the level where physical characteristics of the bottom reach a critical limit beyond which contact with a ship's keel causes either damage or unacceptable effects on controllability and manoeuvrability* [PIANC, 1997].

Nowadays the nautical bottom concept is applied worldwide by several waterways authorities responsible for harbours and access channels suffering from fluid mud sedimentation. In the harbour of Zeebrugge, Belgium, the nautical bottom is theoretically linked to the rheological transition level. However, frequent monitoring of dredging works and updating of nautical charts requires continuous survey methods; unfortunately, up till present the latter are not available for measuring rheological properties. Therefore, for practical reasons the operational definition of the nautical bottom is linked to a critical density value, as continuous density gauges have been developed (e.g. *Navitracker®*, [De Vlieger, 1987]). During a measurement campaign in the 1980s the rheological transition in Zeebrugge always occurred at a density which was higher than 1150 kg/m³, so that the latter was consequently used as a safe critical limit. Other harbours use different values, depending on the local properties of the mud layer, e.g. Cayenne: 1270 kg/m³, Rotterdam: 1200 kg/m³.

A more recent measurement campaign in 1997 revealed that the rheological transition in Zeebrugge occurred at a density level significantly above the current critical density of 1150 kg/m³; on the other hand, the thickness and viscosity of the mud layer above this transition appeared to have increased significantly. A review of the critical density level would have been a logical measure; on the other hand, this would result into more frequent and deeper penetrations of the ship's keel into the mud layer, with possible unacceptable effects on manoeuvrability. As little was known on the manoeuvrability of deep drafted ships in such conditions an extensive research project had been set up at Flanders Hydraulics Research, the hydraulic research station of the Waterways and Maritime Affairs Administration of the Ministry of Flanders, with the scientific support of the Maritime Technology Division of Ghent University. The research program included captive manoeuvring tests, fast-time and full mission bridge simulation runs.

2   Experimental program

2.1   Facilities

To carry out captive manoeuvring tests Flanders Hydraulics Research has a towing tank for manoeuvres in shallow water (88 m * 7 m * 0.6 m) at its disposal. The tank is equipped with a planar motion mechanism with fully automated control and data acquisition system, so that the facilities can be run 24 hours a day, 7 days a week.

Two full mission bridge simulators are available for research and training in confined and shallow navigation areas such as access channels and harbours: SIM225 with a visual system of 225 degrees view allowing a horizontal or vertical tilt of the image, and SIM360+ with 360 degrees view and lateral view of the ship's hull. Both simulators consist of a mock-up of a ship's bridge with navigation equipment for controlling the vessel, digital instruments, communication equipment, radar, ECDIS, etc. Tug assistance can be simulated as well. In the frame of the present project, the simulation runs were carried out with SIM225.

2.2 Ship models

Three ship models have been selected: two container carriers (D: 6000 TEU; U: 8000 TEU) and a tanker model (E). All ship models were equipped with a single propeller and a single rudder. The main characteristics of the models are resumed in Table 1. In this paper only results of ship model D, the 6000 TEU container carrier model, will be discussed, as the most comprehensive captive model test program has been carried out with this ship model, being a typical ship calling at Zeebrugge harbour.

Table 1. Ship models.

Model	D	E	U	Model	D	E	U
Scale	1/75	1/75	1/80	A_R (m²)	60.96	98.34	83.13
L_{PP} (m)	289.8	286.8	331.8	# blades	5	5	6
B (m)	40.25	46.77	42.82	D_P (m)	8.145	7.733	8.46
T (m)	13.50	15.50	14.54	P/D (-)	0.97	0.65	1.00
C_B	0.59	0.82	0.65	AEP (-)	0.8	0.62	0.96

2.3 Bottom conditions

Mud has been simulated using a mixture of two types of chlorinated paraffin and petrol. The characteristics of the different artificial mud layers are shown in Table 2. A mud layer configuration is defined by two characters: a letter (b,…,h) denoting the material characteristics and a figure (1, 2, 3) representing the layer thickness.

Table 2. Bottom conditions and tested models.

Mud type	Density (kg/m³)	Dynamic viscosity (Pa s)	Layer thickness		
			0.75 m "1"	1.50 m "2"	3.00 m "3"
"d"	1100	0.03	D/E	D/E	D/E/U
"c"	1150	0.06	D	D	D
"b"	1180	0.10	D	D	D
"f"	1200	0.11	-	D	-
"h"	1210	0.19	D/E	D/E	D
"e"	1260	0.29	-	D	-
"g"	1250	0.46	-	D/E	D/E
"S"	solid bottom				

The towing tank was covered with a poly-ethylene coating as a protection against the artificial mud. Also the tank had been divided into three sections: a test section (length 44 m) and reservoirs for mud and water. The gross under keel clearance relative to the tank bottom was varied between 7 and 32% of draft, yielding -12 to +21% ukc relative to the mud-water interface. Throughout this paper, the under keel clearance will be expressed with the interface water-mud as a referenc, unless specified otherwise.

2.4 Test types

As the simulation of realistic harbour manoeuvres is one of the main purposes of the research program, sufficient model test data had to be available to simulate a wide range of possible manoeuvres. The captive manoeuvring program consisted of bollard pull tests with varying rudder angle and propeller rate; stationary tests with varying forward speed, rudder angle, drift angle and propeller rpm; harmonic sway and yaw tests; multimodal tests with variable speed, rudder angle or propeller rpm. The speed of the vessels was varied between 2 knots astern and 10 knots ahead.

Following data were measured: longitudinal and lateral force components fore and aft, vertical motion (4 measuring posts: fore/aft, port/starboard), rudder parameters (normal and tangential forces, torque, angle), propeller parameters (torque, thrust, rpm). In particular cases, vertical motions of the mud-water and water-air interfaces were registered as well.

3 Mathematical modelling

3.1 Modelling methods

The proposed mathematical model attempts to take account of the physical background of the hydrodynamic forces as much as possible. A modular model has been developed, in which hull (H), propeller (P) and rudder (R) induced forces have been modelled separately and are then joined using correlation parameters. Rather than attempting to fit the data with analytical functions, the model results are given in tabular format, interlaying points being calculated by linear interpolation. The coefficients of the model are bottom dependent, so during the simulator runs the bottom conditions were supposed to be stationary. In future, efforts will be taken to include varying bottom conditions in one run.

3.2 Hull forces

3.2.1 Longitudinal force

The longitudinal hull force is as given by:

$$X_H = \left(X_{\dot{u}}\left(u\right) - m\right)\dot{u} + mvr + mx_G r^2 + \left[X_{\dot{v}\dot{v}}\left(u\right)\dot{v}^2 + X_{\dot{v}}\left(u\right)\dot{v} + X_{\dot{r}\dot{r}}\left(u\right)\dot{r}^2 + X_{\dot{r}}\left(u\right)\dot{r}\right]$$
$$+ \tfrac{1}{2}\rho LT\left\{\left(u^2 + v^2\right)\left(X'(\beta)\right) + \left(u^2 + \left(\tfrac{1}{2}rL\right)^2\right)X'(\gamma) + \left(v^2 + \left(\tfrac{1}{2}rL\right)^2\right)X'(\chi)\right\} \tag{1}$$

Velocity dependent terms are modelled with tabular functions of the drift angle β, the yaw rate angle γ and a correlation angle χ. A point of interest is the dependence on the accelerations. Usually the longitudinal force will only be affected by longitudinal accelerations. However, in case of contact between the ship's keel and high density mud (>1200 kg/m³), sway and yaw acceleration also have a significant influence. Moreover, the speed-force relation appears to be no longer quadratic, so that for each speed a separate tabular function must be introduced. In all other cases those influences are unimportant. Figure 1 shows the non-dimensional resistance at a speed of 2 knots. Touching high density mud layers leads to a dramatic increase of resistance.
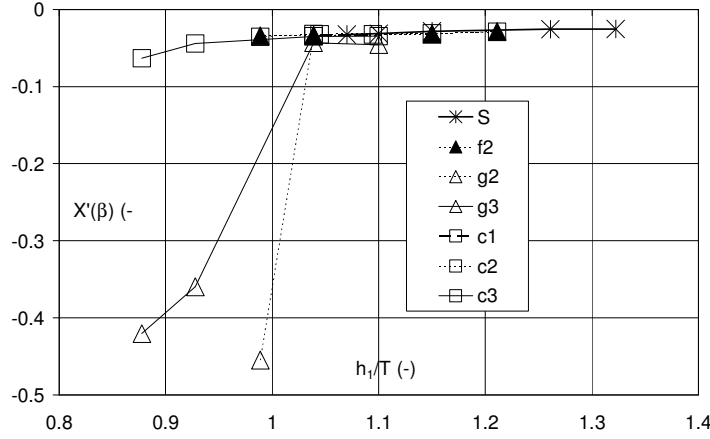

Fig. 1. Ship resistance: influence of bottom characteristics and ukc at low speed.

3.2.2 Sway force and yawing moment

The proposed model for the sway force is given by:

$$Y_H = \left(Y_{\dot{v}} - m\right)\dot{v} + \left(Y_{\dot{r}}\left(\beta\right) - mx_G\right)\dot{r} - mur + \tfrac{1}{2}\rho LT\left\{\begin{array}{c}\left(u^2 + v^2\right)Y'(\beta) + \left(u^2 + \left(\tfrac{1}{2}rL\right)^2\right)Y'(\gamma) \\ + \left(v^2 + \left(\tfrac{1}{2}rL\right)^2\right)Y'(\chi)\end{array}\right\} \tag{2}$$

The hydrodynamic inertia increases significantly in muddy navigation areas. As an example, Figure 2 shows the sway added mass. Drift and yaw induced forces also increase with decreasing ukc. The yawing moment is modelled as:

$$N_H = \left(N_{\dot{v}} - mx_G\right)\dot{v} + \left(N_{\dot{r}}\left(\beta\right) - I_{zz}\right)\dot{r} - mx_G ur + \tfrac{1}{2}\rho L^2 T\left\{\begin{array}{c}\left(u^2 + v^2\right)N'(\beta) + \left(u^2 + \left(\tfrac{1}{2}rL\right)^2\right)N'(\gamma) \\ + \left(v^2 + \left(\tfrac{1}{2}rL\right)^2\right)N'(\chi)\end{array}\right\}$$
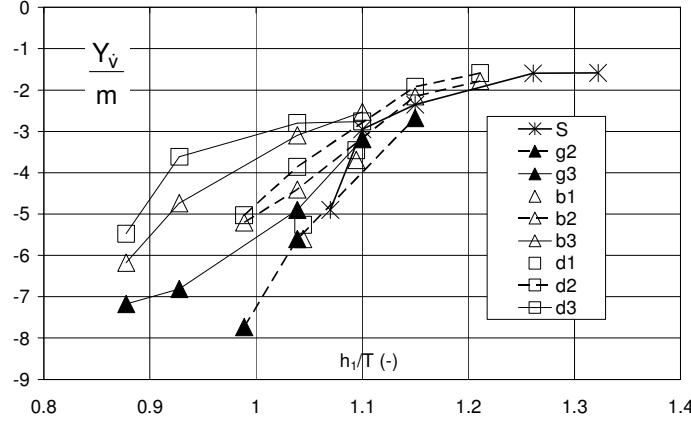$$\tag{3}$$

Fig. 2. Sway added mass: influence of bottom characteristics and ukc.

The effect of mud layers on the yawing moment is analogue as with the sway force. In general the components of Y_H and N_H in muddy areas can be seen as an extrapolation of the forces in the shallow water domain.

3.3 Propeller forces

3.3.1 Thrust and torque

The thrust coefficient C_T and the torque coefficient C_Q are available for each propeller in open water conditions and are given in function of the hydrodynamic angle ε:

$$\varepsilon = \arctan\left(\frac{u_P}{0.7\pi\, nD_P}\right) = \arctan\left(\frac{u(1-w)}{0.7\pi\, nD_P}\right) \tag{4}$$

in which u_P represents the advance speed of the propeller:

$$u_P = (1-w)u \tag{5}$$

with w the wake factor formulating the relationship with u, the forward speed of the ship. A different wake factor is calculated for the thrust and the torque. The wake factor is given in function of the apparent hydrodynamic angle ε^*:

$$\varepsilon^* = \arctan\left(\frac{u}{0.7\pi nD_P}\right) \tag{6}$$

The wake factor w_T for the thrust, which is represented on Figure 3, is significantly higher when navigating in muddy areas of a low density. This effect can be related to the undulations in the water-mud interface, which increase and move more aft with increasing speed and decreasing mud density. With low density mud layers, the undulations are maximal near the propeller and disturb the propeller inflow.

The wake factor for the torque takes high values in contact with high density mud layers, due to the fact that the blade tips are moving through the mud, yielding a larger torque. The combination of a large torque and an increased resistance results in a very poor propeller efficiency when the ship penetrates a mud layer.
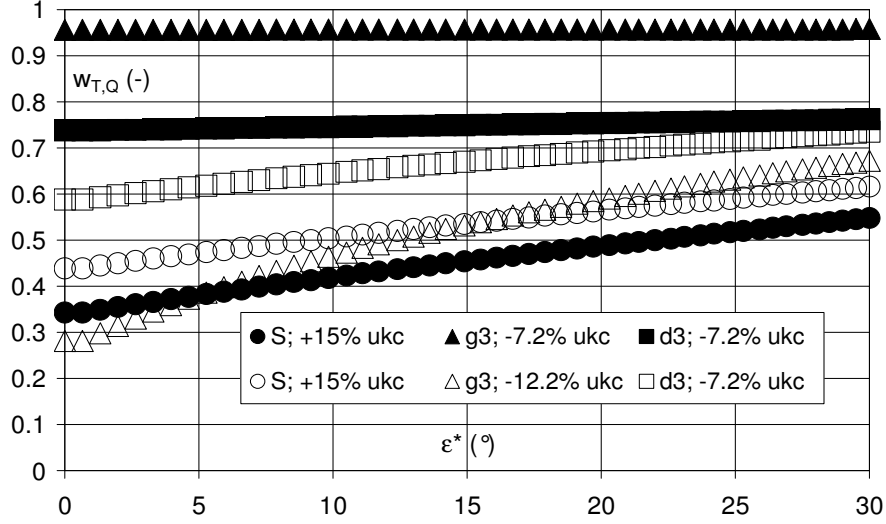

Fig. 3.   Wake factor for thrust (transparent symbols) and torque (filled symbols). Influence of bottom conditions.

3.3.2   Propeller induced forces

The propeller induces a longitudinal force X_P on the hull, which is only a fraction of the thrust T_P; as usual, this effect is modelled by means of the thrust deduction factor t. t increases with decreasing propeller loading and is larger in muddy navigation areas.

Flow asymmetry around the propeller a lateral force and a yawing moment. In the 2nd and 4th quadrant, the ship velocity and the propeller rate are opposite, resulting in eddies near the stern and oscillating forces and moments:

$$Y_P = \left|\frac{n}{n_0}\right|\left(Y_{\dot{v}}^n \dot{v} + Y_{\dot{r}}^n \dot{r}\right) + \begin{bmatrix} K_1\left[Y_{PT}(\beta,\varepsilon*) + Y_{PT}(\gamma,\varepsilon*)\right] + \\ K_2\left[Y_{PTA}(\beta,\varepsilon*)\right]\left[\cos\left(\omega(\beta,\varepsilon*)t + j(\beta,\varepsilon*)\right)\right] \end{bmatrix} T_P(\varepsilon*) \qquad (7)$$

$$N_P = \left|\frac{n}{n_0}\right|\left(N_{\dot{v}}^n \dot{v} + N_{\dot{r}}^n \dot{r}\right) + \begin{bmatrix} \left[N_{PT}(\beta,\varepsilon*) + N_{PT}(\gamma,\varepsilon*)\right] + \\ \left[N_{PTA}(\beta,\varepsilon*,K_2)\right]\left[\cos\left(\omega(\beta,\varepsilon*)t + j(\beta,\varepsilon*)\right)\right] \end{bmatrix} L_{PP}T_P(\varepsilon*) \qquad (8)$$

K_1 and K_2 are quadrant depending: $K_1 = F_n$ in quadrant 1 and equals 1 in other quadrants; $K_2 = 1$ in quadrants 1, 2, 3 and takes a value between 0 and 1 in quadrant 4. Figure 4 shows as an example the average lateral force due to propeller action in the

first quadrant. An increase of the asymmetry force can be observed in muddy areas, especially with positive ukc. Also the difference between port and starboard, due to the right handed propeller which the ship was equipped with, increases in muddy areas, as well as the amplitude of the oscillations.
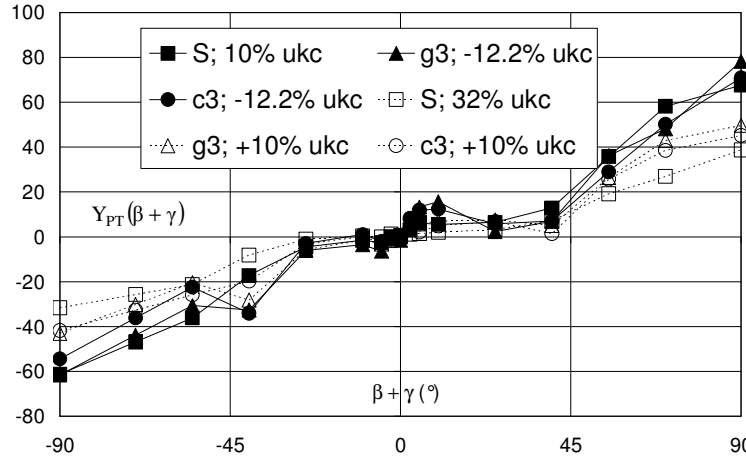

Fig. 4.   Average lateral force due to propeller action (1st quadrant): influence of bottom characteristics.

3.4   Rudder forces

3.4.1   Forces acting on the rudder

Open water drift and lift coefficients (C_D, C_L) are available for a 360 deg range of rudder attack angles α_R . The longitudinal and lateral rudder forces are modelled as:

$$F_X = \tfrac{1}{2}\rho A_R V_R^2 \left[C_L\left(\alpha_R\right)\sin\beta_R + C_D\left(\alpha_R\right)\cos\beta_R \right]$$

$$F_Y = \tfrac{1}{2}\rho A_R V_R^2 \left[C_L\left(\alpha_R\right)\cos\beta_R - C_D\left(\alpha_R\right)\sin\beta_R \right]$$

(9-10)

in which β_R represents the drift angle of the flow near the rudder. The longitudinal inflow velocity at the rudder depends on the ship's speed and the propeller loading. To model the latter, the impulse theory has been used. The effect of the hull is modelled using a wake factor, which has an analogue definition as in eqn (5). As with the wake factor for the thrust, a larger wake is observed in low density muddy areas, which again can be explained by undulations of the water-mud interface near the stern.

3.4.2   Rudder induced forces

The longitudinal rudder force yields an extra resistance X_R on the ship's hull. X_R does not seem to be significantly different from F_X, so that both are modelled in the same way. The asymmetric flow induced by the rudder not only results in a lateral force F_Y on the rudder (with application point x_R), but also in an extra lateral force $a_H F_Y$ (with application point x_H) due to an asymmetric flow around the hull. This leads to:

$$Y_R = (1 + a_H) F_Y \tag{11}$$

$$N_R = (x_R + a_H x_H) F_Y \tag{12}$$

In the first quadrant a_H reaches a maximum at a certain propeller loading, which is noticeably lower above solid bottoms. In self-propelled conditions a_H increases with decreasing under keel clearance and decreasing layer thickness. In the 4th quadrant a different effect is observed. For positive under keel clearances, a_H lies between 0 and -1, but when the ship's keel is near the interface, a_H is more or less -1. In this case the rudder has no effect upon the hull. With even smaller ukc the rudder induces an opposite effect. The application point x_H moves to amidships with decreasing ukc.

4   Simulation runs

The simulation program had to meet three objectives:

1. Validation of the mathematical model, by simulations in situations the pilots are familiar with, such as a solid bottom.
2. Defining the limit of controllability: a selection of conditions with small negative under keel clearance to define the nautical bottom.
3. Assessing the navigability in contact with mud layers. Adopting a larger critical limit will lead to contact between the ship's keel and mud layers of a lower density. A number of those conditions has been selected as well.

For the assessment of the runs, the following criteria have been taken into account:

1. Speed. Can the vessel, when leaving the harbour, develop sufficient speed to counteract the currents outside the breakwaters?
2. Is the course stability sufficient? The standard deviation on the yaw rate of the ship seemed a suitable evaluation parameter.
3. Are the ship's own controls and the offered tug assistance S sufficient to carry out the manoeuvres safely and in an economic way? The controllability has been evaluated by analysing the impulse of steering force and moment, defined by:

$$I_Y = I_{YT} + I_{YR} = \sum_i \int S_i dt + \int |Y_R| dt \ ; \ I_N = I_{NT} + I_{NR} = \sum_i \int S_i x_i dt + \int |N_R| dt \tag{13-14}$$

The result of this analysis is presented in Figure 5, valid in case the ship is assisted by two tugs of 45 ton bollard pull. Based on the results of the real-time simulations, the critical density of the harbour of Zeebrugge can be increased to 1200 kg/m³. However, the penetration depth into mud layers of lower density should be subject to restrictions. The analysis of the results also revealed the importance of tug assistance. More tug power reduces the constraint of navigability in contact with lower density mud layers, but does not affect the definition of the nautical bottom. If less tug power is available, the mud-water interface should be considered as the nautical bottom.
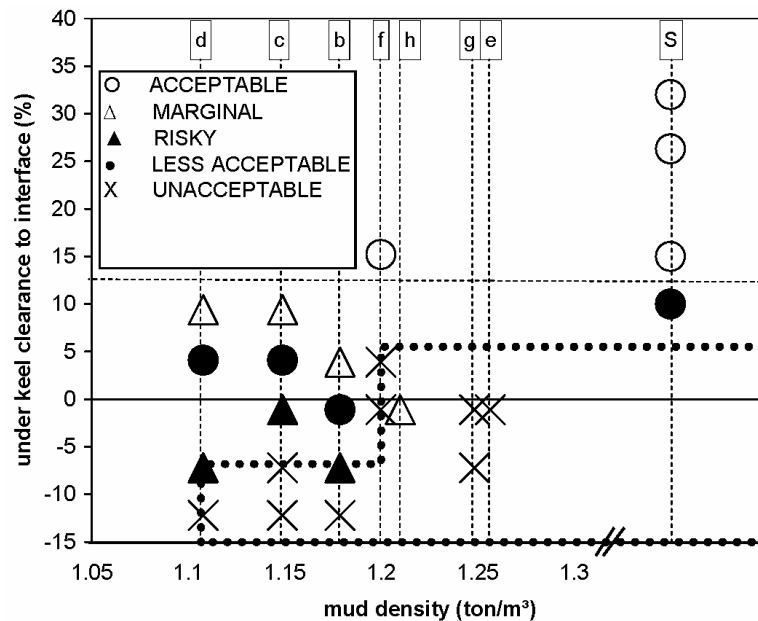
Fig. 5. Ship D, real time simulations. Quantitative evaluation of all criteria with assistance by two tugs of 45 ton bollard pull (dotted area = "unacceptable").

Acknowledgements

References

De Vlieger H., De Cloedt J. (1987): Navitracker: a giant step forward in tactics and economics of maintenance dredging, Terra et Aqua, No. 35, pp. 2 – 18.

PIANC (1997): Approach channels – A guide for design, Final report of the joint Working Group PIANC and IAPH, in cooperation with IMPA and IALA. Supplement to PIANC Bulletin, No. 95, 108 pp.